HHS Public Access

Author manuscript

Neurobiol Dis. Author manuscript; available in PMC 2022 February 07.

Published in final edited form as:

Neurobiol Dis. 2018 June ; 114: 174–183. doi:10.1016/j.nbd.2018.03.002.

Antisense-Mediated Reduction of EphA4 in the Adult CNS Does Not Improve the Function of Mice with Amyotrophic Lateral Sclerosis

Karen K. Ling[a], **Michaela Jackson**[a], **Duah Alkam**[b], **Dawei Liu**[f], **Norm Allaire**[f], **Chao Sun**[f], **Mahmoud Kiaei**[b,c,d,e], **Alexander McCampbell**[f], **Frank Rigo**[*,a]

[a]Ionis Pharmaceuticals, Carlsbad, CA, USA

[b]Department of Neurology, University of Arkansas for Medical Sciences, Little Rock, AR, USA

[c]Department of Pharmacology and Toxicology, University of Arkansas for Medical Sciences, Little Rock, AR, USA

[d]Center for Translational Neuroscience, University of Arkansas for Medical Sciences, Little Rock, AR, USA

[e]Department of Geriatrics, University of Arkansas for Medical Sciences, Little Rock, AR, USA

[f]Biogen, Cambridge, MA, USA

Abstract

Amyotrophic lateral sclerosis (ALS) is a fatal adult onset motor neuron disease characterized by progressive denervation and subsequent motor impairment. EphA4, a negative regulator of axonal growth, was recently identified as a genetic modifier in fish and rodent models of ALS. To evaluate the therapeutic potential of EphA4 for ALS, we examined the effect of CNS-directed EphA4 reduction in preclinical mouse models of ALS, and assessed if the levels of *EPHA4* mRNA in blood correlate with disease onset and progression in human ALS patients. We developed antisense oligonucleotides (ASOs) to specifically reduce the expression of EphA4 in the central nervous system (CNS) of adult mice. Intracerebroventricular administration of an Epha4-ASO in wild-type mice inhibited *Epha4* mRNA and protein in the brain and spinal cord, and promoted re-innervation and functional recovery after sciatic nerve crush. In contrast, lowering of EphA4 in the CNS of two mouse models of ALS ($SOD1^{G93A}$ and $PFN1^{G118V}$) did not improve their motor function or survival. Furthermore, the level of *EPHA4* mRNA in human blood correlated weakly with age of disease onset, and it was not a significant predictor of disease progression as measured by ALS Functional Rating Scores (ALSFRS). Our data demonstrates that lowering EphA4 in the adult CNS may not be a stand-alone viable strategy for treating ALS.

[*]Corresponding author. Postal address: 2855 Gazelle Ct., Carlsbad, USA. frigo@ionisph.com.

Disclosure statement

All authors have seen and approved the final version of the manuscript being submitted. KKL, MJ and FR are paid employees of Ionis Pharmaceuticals, Inc. DL, NA, CS and AM are employees of Biogen, Inc. DA and MK declare that they have no competing interests.

Keywords

Amyotrophic lateral sclerosis; Ephrin receptor A4; antisense oligonucleotides; superoxide dismutase 1; profilin 1

Introduction

Amyotrophic lateral sclerosis (ALS) is primarily an adult onset neurodegenerative disease in which upper and lower motor neurons degenerate leading to paralysis and death 2–5 years after diagnosis. About 10% of the ALS population inherits the disease. *SOD1*, *TARDBP*, *FUS* and C9ORF72 are among the most common ALS-causing genes accounting for ~70% of familial and ~10% of sporadic ALS (Al-Chalabi et al., 2017; Renton et al., 2014; Taylor et al., 2016). Mutations in these genes are thought to cause disease by an RNA and/or protein gain-of-function mechanism (Taylor et al., 2016). RNA-targeted therapeutics such as siRNA or antisense oligonucleotides (ASOs) that reduce the production of toxic RNA and/or protein are ideally suited for treating familial forms of ALS (Reddy and Miller, 2015). However, most sporadic ALS has no clear genetic basis and strategies other than targeting ALS genes are necessary. Given that muscle denervation is key to the progressive loss of motor function and eventual paralysis in all forms of ALS, therapeutic strategies that promote axonal growth and reinnervation may present a sensible approach to treat ALS.

Recently, *EPHA4*, a gene known to play a role in axonal remodeling, was identified as a genetic modifier of ALS in animal models and humans (Van Hoecke et al., 2012). *EPHA4* encodes Ephrin receptor A4 (EphA4), a tyrosine kinase receptor that interacts with membrane-tethered ligand ephrins at cell-cell interfaces. This promotes important cellular process, such as cell migration and axonal guidance. During development, EphA4 is crucial for proper pathfinding of corticospinal as well as sensory axons (Klein and Kania, 2014). EphA4 binds to its high-affinity ligand ephrin at cell-cell interfaces and induces rapid internalization of the receptor and activation of RhoA-ROCK signaling. This reduces cell-cell adhesion and increase growth cone motility (Goldshmit et al., 2004; Klein, 2012; Lowery and Van Vactor, 2009; Murai and Pasquale, 2005). In the adult CNS, activation of EphA4 receptor induces spine retraction while inhibition leads to disorganization of dendritic spines implicating its role in synaptic plasticity (Lai and Ip, 2009; Murai et al., 2003a). In the injured CNS, ephrins and EphA4 are upregulated (Frugier et al., 2012; Goldshmit et al., 2006) restricting axonal regeneration after injury. Blockade of the EphA4 promotes axonal regrowth and functional recovery in optic nerve injury, spinal cord injury and stroke models (Goldshmit et al., 2004; Goldshmit et al., 2011; Joly et al., 2014; Overman et al., 2012). In the context of ALS, genetic or pharmacological inhibition of EphA4 rescues axonal defects caused by mutations in ALS-associated genes (*SOD1* and *TDP43*) in zebrafish, and promotes motor function and prolongs survival in *SOD1* mouse models of ALS (Van Hoecke et al., 2012). In addition, it has been reported that in humans with ALS, EphA4 expression is inversely correlated with disease onset and lifespan (Van Hoecke et al., 2012). As a whole, the data suggests that blocking EphA4 expression should promote axonal growth, reinnervation and motor function in patients with ALS (Faruqi, 2012).

In this study, we determined if EphA4 is a good pharmacological target for ALS. First, we evaluated the function of EphA4 in promoting axonal regeneration. Then we determined if pharmacological inhibition of *Epha4 mRNA* with ASOs resulted in phenotypic improvements in two mouse models of ALS ($SOD1^{G93A}$ and $PFN1^{G118V}$) that recapitulate many features of ALS (Fil et al., 2017; Gurney, 1997; Gurney et al., 1994). Finally, we re-assessed the relationship of *EPHA4* mRNA in blood with age of ALS onset in humans. Here we report that lowering *Epha4* expression in the CNS promotes axonal regeneration and motor function recovery in peripheral nerve crush injury, however, it does not improve motor function or survival in both pre-clinical ALS mouse models. Furthermore, we confirmed a weak inverse relationship between age of onset and expression level of *EPHA4* mRNA in blood, which nonetheless was not a significant predictor of ALSFRS progression.

Results

Epha4-ASO efficiently reduces *Epha4* mRNA and protein in the adult mouse CNS

We have previously shown that intracerebroventricular (ICV) administration of gapmer ASOs which harness the RNase H mechanisms achieve widespread distribution and target reduction in the CNS of mice (DeVos et al., 2013; DeVos et al., 2017; Kordasiewicz et al., 2012). We identified RNase H ASOs that efficiently reduce the expression of *Epha4* mRNA in cultured cells (data not shown), and tested the most potent ones for target reduction in the CNS of mice. To achieve knockdown of *Epha4* mRNA in the CNS of mice, we administered Epha4-ASO1 to adult mice by ICV bolus injection. Two weeks after the injection, we observed a ~70% reduction of *Epha4* mRNA in the spinal cord (Fig. 1A) and cortex (Fig. 1B), and a similar reduction was achieved using Epha4-ASO2 (Supplementary Fig. S1). This reduction was sustained for over 6 weeks. Furthermore, EPHA4 protein was also reduced in the CNS (Fig. 1C).

Epha4-ASO improves NMJ re-innervation and functional recovery after sciatic nerve injury

To determine if the reduction of EphA4 promotes peripheral nerve regeneration, we suppressed *Epha4* expression with ASOs and analyzed structural and functional recovery of the tibialis anterior muscle after traumatic nerve injury. We used the sciatic nerve crush model, which has been used extensively for studying peripheral nerve regeneration (Geuna et al., 2016). To ensure robust *Epha4* mRNA reduction during the short window of time where regeneration occurs, Epha4-ASO1 or -ASO2 were injected into the CNS of mice 2 weeks prior to crushing the sciatic nerve (Fig. 2A). Innervation of neuromuscular junctions (NMJs) was examined by immunostaining: post-synaptic specializations and pre-synaptic nerve terminals were visualized by staining for α-bungarotoxin or α-BTX (red) and vesicular acetylcholine transporter or VAChT (green), respectively. Three days after the nerve crush, all NMJs were denervated (data not shown). Thirteen days after crushing the nerve, the majority (~90%) of NMJs remained denervated in mice that were not treated with ASO (Fig. 2B). In contrast, the muscle of mice that had been treated with the Epha4-ASOs showed an increase in innervated NMJs as demonstrated by the superposition of the pre- and post-synaptic counterparts which appeared yellow (Fig. 2B). Quantification of NMJs stained

with both α-BTX and VAChT showed that 40% of NMJs were innervated in ASO treated mice compared to ~10% in vehicle treated group (Fig. 2C).

To determine if the increased ASO-mediated re-innervation was associated with a functional recovery, we measured the grip strength of the limb that was innervated by the damaged nerve. Vehicle-treated mice gradually regained their grip strength over the course of 4 weeks after the nerve crush (Fig. 2D). Mice treated with the Epha4-ASO1 showed a faster recovery in their grip strength (two-way ANOVA, $p = 0.0467$). Together, these results suggest ASO-mediated *Epha4* reduction in the CNS of adult mice and promotes re-innervation of NMJs that lead to functional recovery in the context of peripheral nerve injury.

Epha4-ASO treatment does not affect body weight, disease progression, survival, and motor performance of SOD1^{G93A} mice

Given the pronounced improvement in sciatic nerve regeneration we observed after reducing *Epha4* expression in the adult CNS, we asked if lowering *Epha4* improves nerve regeneration and the function and survival of ALS mice as previously reported (Van Hoecke et al., 2012). Epha4-ASO1 or -ASO2 were delivered by ICV bolus injection to SOD1^{G93A} mice at 7 weeks of age, before overt neurological or motor phenotypes are typically observed. A second dose of ASO was given at 13 weeks of age to ensure robust *Epha4* mRNA reduction throughout the disease course (Fig. 3A). SOD1^{G93A} mice treated with the Epha4-ASOs attained their peak body weight (~25 g) at ~120 days, as did the vehicle treated mice (Fig. 3B). Both the Epha4-ASO-treated groups and vehicle-treated mice displayed rapid body weight loss and showed a 10% body weight loss at ~150 days old. Therefore, lowering of *Epha4* expression did not ameliorate the weight loss of SOD1^{G93A} mice (Fig. 3C and D).

To determine if lowering of *Epha4* expression delayed disease onset, we assessed whether Epha4-ASO treated SOD1^{G93A} mice showed an improvement in the splay reflex and hindlimb clasping, tests that detect early motor deficits in this disease model (Gurney et al., 1994; Hatzipetros et al., 2015). We observed no improvement in the onset of disease in Epha4-ASO treated mice compared to vehicle-treated mice (Fig. 3E). In addition, Epha4-ASO treatment had no effect on the disease progression and survival of SOD1^{G93A} mice (Fig. 3F & G).

We examined the motor function of SOD1^{G93A} mice treated with Epha4-ASOs by testing their performance on the rotarod. At all time-points tested, the Epha4-ASO1 treated mice showed a latency to fall from the rotarod comparable to vehicle-treated mice (Fig. 3H). In addition, we measured the compound muscle action potential (CMAP) to assess the functional status of the motor unit pool (Fig. 4A). At the time of ASO treatment (5 weeks of age), the CMAP of SOD1^{G93A} mice was indistinguishable from the WT littermates. The CMAP of Epha4-ASO1 treated mice declined at the same rate as for the vehicle-treated SOD1^{G93A} mice (Fig. 4B). Given that ASO treatment achieved a robust decrease of *Epha4* mRNA in the cortex and spinal cord (including motor neurons) of SOD1^{G93A} mice (Fig. 3I, 4C, Supplementary Fig. S2 and S3), altogether our data indicates that *Epha4* reduction in the CNS of adult SOD1^{G93A} mice does not result in a significant amelioration of disease phenotypes.

Epha4-ASO treatment improves disease onset but not survival or motor function in PFN1^{G118V} mice

To determine if our observations were unique to the SOD1^{G93A} mouse model, we also tested the effects of *Epha4* lowering in another mouse model of ALS that has a mutation in the Profilin1 (*PFN1*) gene (Fil et al., 2017). Briefly, the PFN1^{G118V} transgenic mice overexpressing mutant human PFN1 protein exhibits an array of phenotypes and pathologies found in ALS patients, including upper and lower motor neuron loss, axonal degeneration, denervation, muscle atrophy, progressive motor dysfunction with the onset of symptoms at P150 days and rapid progression to paralysis and death at disease end-stage ranging from P175 to 280 days (Fil et al., 2017). Since ALS-associated *PFN1* mutations shunts axon outgrowth in vitro (Wu et al., 2012) and causes axonal degeneration in vivo (Fil et al., 2017), and EphA4 inhibition was shown to promote axonal growth (Goldshmit et al., 2006), we asked if EphA4 inhibition could reverse the ALS-like phenotypes in the PFN1^{G118V} mutant mice. We administered one dose of ASO at post-natal day ~50 and a second dose at post-natal day 114, and the mice were examined as was done for the SOD1^{G93A} mice. We analyzed the average and median age at which the animals had 10% weight loss (Fig. 5A–C) and found that Epha4-ASO1 treatment did not significantly delay weight loss compared to control ASO-treated mice (median age of Epha4-ASO vs CNTL-ASO: 193.5 vs 186 days, Kaplan-Meier, $p = 0.429$). Interestingly, Epha4-ASO1 treatment delayed the onset of neurological symptoms of the PFN1^{G118V} mutant mice (Fig. 5D; 199 days for the Epha4-ASO1 and 154 days for the CNTL-ASO). However, Epha4-ASO1 treatment did not improve the survival of mutant mice (Fig. 5F), and the disease progressed faster (Fig. 5E) without measurable improvement in motor function as determined by performance on the rotarod, stride length and CMAP (Fig.6A–C). Additionally, we checked glial fibrilary acidic protein (GFAP, a marker of astrocytosis) in the spinal cord and cytochrome-c oxidase isoform 4 (COX4, a marker of mitochondria) levels in gastrocnemius muscle as pathological biomarkers. We found no significant reduction in GFAP levels by western blot (supplementary materials, Fig. S4A) and no significant increase in COX4 levels in the gastrocnemius muscles of Epha4-ASO1 treated animals (supplementary materials, Fig. S4B). Therefore, a robust reduction of both *Epha4* mRNA and protein in the CNS of ASO-treated animals (Fig. 6D and E) does not improve disease phenotypes and survival of mice with ALS.

EPHA4 mRNA in whole blood is associated with age of ALS onset

Prior work had suggested that there is an inverse relationship between *EPHA4* expression in total blood and age of ALS onset (Van Hoecke et al., 2012). We assessed this relationship in an independent collection of blood samples from 187 ALS patients. Subject demographics were representative of ALS patient populations, with 65% male and 35% female individuals and a mean age of disease onset of 51.9 years (Table 1). We confirmed a weak inverse relationship between age of onset and expression level of *EPHA4* mRNA in blood (Fig 7, $p < 0.05$, $R^2 = 0.026$). We also assessed the ability of *EPHA4* levels in the blood to predict rate of disease progression measured by ALS Functional Rating Scores (ALSFRS). While baseline ALSFRS, symptom duration, and age of onset were significant predictors of ALSFRS progression, *EPHA4* levels were not (Table 2).

Discussion

Our results show that Epha4-ASO effectively reduces *Epha4* mRNA and protein after single bolus ICV injection into adult mouse CNS. Administration of Epha4-ASO in wild type mice promotes reinnervation and functional recovery in response to injury supporting the role of EphA4 as a negative regulator of axon regeneration after acute injury (Goldshmit et al., 2006; Goldshmit et al., 2011; Joly et al., 2014; Van Hoecke et al., 2012). However, in the context of ALS, Epha4-ASO injection in transgenic mice carrying mutant *SOD1* or *PFN1* genes at pre-symptomatic ages (35–50 days) did not preserve motor function evaluated by both electrophysiological and behavioral endpoints, or improve survival of mouse models of ALS. In conclusion, our data supports *EPHA4* as a target to promote axonal regeneration in traumatic nerve injury, but targeting *EPHA4* in the CNS may not be an effective therapeutic strategy for the treatment of ALS.

It has been reported that genetic or pharmacological inhibition of EphA4 corrects ALS phenotypes in zebrafish and rodent ALS models. The lack of therapeutic effect of EphA4 suppression observed in this study is in stark contrast with the previous report (Van Hoecke et al., 2012). There are several potential explanations for the apparent discrepancy. The previous study undertook a genetic approach to remove EphA4 receptors by crossing $SOD1^{G93A}$ mice with mice carrying a spontaneous germline mutation in *Epha4* gene. The double mutant (*Epha4 +/−; SOD1*^{G93A}) is expected to have a 50% loss of EPHA4 protein throughout development, well before ALS symptom onset. In contrast, in our study, ASO-mediated suppression of *Epha4* mRNA and protein in the adult CNS may not have occurred early enough to exert its protective effect. Alternatively, in the previous genetic approach, EphA4 expression was reduced in the CNS and the periphery compared to our study where reduction of EphA4 expression was confined to the CNS. Perhaps inhibiting EphA4 expression in the CNS alone is not sufficient for improving the phenotype of mice with ALS.

Van Hoecke et al. showed previously that a continuous infusion of an EphA4 blocking peptide (KYL) in the cerebroventricular space of adult $SOD1^{G93A}$ rats improved their motor function and survival, suggesting that adult CNS is the major target tissue. However, the KYL peptide also has lower affinity towards other Ephrin type A and B receptors (Murai et al., 2003b), and their partial inhibition may have contributed to the phenotypic improvements observed. More intriguingly, a recent study reported that a brain-penetrating selective EphA4 agonist extends the survival of *SOD1*^{G93A} mice (Wu et al., 2017). Several mechanisms, that are not mutually exclusive, may explain the beneficial effect on survival. These include: 1) activation of EphA4 and its forward signaling; 2) reduced surface receptor activity via ligand-induced receptor internalization, and; 3) reducing the reverse signaling of ephrins on astrocytes. Antisense-mediated reduction of EphA4 is expected to inhibit all EphA4 signaling, and our data supports the hypothesis that a more complex signaling mechanism, rather than EphA4 inhibition itself, may mediate the protective effect observed with peptide mimetics.

EPHA4 mRNA in the blood cells was reported to correlate with disease onset (Van Hoecke et al., 2012). Our findings replicate this initial observation in a second cohort of ALS

patients. The strength of the association appears to be more modest, though our patient cohort has fewer very young ALS patients than in the initial report. One limitation of our analysis is the lack of healthy normal controls. *EPHA4* transcript levels appear to decrease with age in the peripheral blood and possibly frontal cortex during normal aging (Peters et al., 2015). Age-related loss of *EPHA4* may be a risk factor for ALS, the risk of which increases with age (Johnston et al., 2006). The lack of association of *EPHA4* with rate of disease progression post onset suggests the age-related changes may by correlative and not causative. Future analysis of EPHA4 in the CSF of ALS patients may provide a more proximal assessment of EPHA4 protein levels in the disease state.

Our work raises the question of whether inhibiting a single extrinsic signal that hinders regeneration is an effective approach to promote regeneration in ALS. Sema 3A and Nogo-A are classic axonal repellents found upregulated in ALS mouse models and in human patients (Bros-Facer et al., 2014; Bruneteau et al., 2015; De Winter et al., 2006; Jokic et al., 2005; Venkova et al., 2014). Inhibiting Nrp1 (a component of Sema 3A receptor) or Nogo-A receptor at early pre-symptomatic age can overcome the axonal inhibition and delay neuromuscular denervation in $SOD1^{G93A}$ mice (Bros-Facer et al., 2014; Jokic et al., 2006; Venkova et al., 2014). However, the beneficial effects are only transient and become less effective over a longer treatment period. Given the compensatory inhibition that has been observed when a single inhibitory molecule was genetically depleted in the CNS (Kempf et al., 2013), modulating a single inhibitory extrinsic signal may not be an effective monotherapy for ALS. In light of the unexpected results in our Epha4-ASO mouse trial as well as the disappointing outcome of a recent ALS clinical trial with the humanized anti-Nogo-A antibody (Meininger et al., 2017), one may need to target multiple inhibitory signals to effectively promote regeneration in ALS.

Although ASO-mediated EphA4 reduction does not improve motor function or survival of ALS mouse models, it does promote reinnervation/recovery after nerve crush. It would be interesting to further evaluate the therapeutic potential of Epha4-ASOs in acute CNS injury, such as spinal cord injury and stroke, in which EphA4 inhibition has been reported to promote regeneration (Goldshmit et al., 2004; Goldshmit et al., 2006; Goldshmit et al., 2011; Joly et al., 2014; Lemmens et al., 2013; Overman et al., 2012).

Materials and methods

Oligonucleotide synthesis.

Synthesis and purification of all chemically modified oligonucleotides were performed as previously described (Swayze et al., 2007). The MOE-gaper ASOs are 20 nucleotides in length, wherein the central gap segment comprising ten 2’-deoxyribonucleotides that are flanked on the 5’ and 3’ wings by five 2’MOE modified nucleotides. Internucleotide linkages are phosphorothioate interspersed with phosphodiester, and all cytosine residues are 5’-methylcytosines.

Animals.

All the animals were housed in animal facility at Ionis Pharmaceuticals and all the procedures performed complied with NIH guidelines and were approved by the Institutional Animal Care and Use Committee at Ionis Pharmaceuticals. $SOD1^{G93A}$ transgenic male mice expressing a G93A mutant form of human *SOD1* transgene [B6.Cg-Tg(SOD1*G93A)1Gur/J; Stock No: 004435] and gender-matched wildtype littermates were obtained from Jackson Labs (Bar Harbor, ME). $PFN1^{G118V}$ transgenic mice overexpressing a G118V variant of human Profilin1 gene and wild type littermates were generated in the Kiaei laboratory as new mouse model of motor neuron disease or ALS (Fil et al., 2017). These mice are now available form Jackson Labs (Bar Harbor, ME) [C57BL/6N-Tg(Prnp-PFN1*G118V)838Kiaei/J Stock No: 030568]. Litter-matched and gender-balanced mouse cohorts were used in the study.

Copy number analysis.

Transgene copy number was quantified using qPCR as previously described (Heiman-Patterson et al., 2005). $SOD1^{G93A}$ transgenic mice with 16–24 copies of transgene were included in the analyses.

Randomization and blinding of animals in treatment groups.

To achieve copy number-matched, gender-matched and litter-matched mice in each treatment group, mice were divided according to transgene copy number, gender and date of birth, and randomly assigned to treatment groups. ASOs were blinded and assigned to treatment groups by an individual who were not conducting the study or the analyses. Treatments were unblinded to the investigator after all analyses were completed.

ASO intracerebroventricular administration.

ASO dissolved in phosphate buffered saline (PBS) was prepared and injected as previously described (Rigo et al., 2014) with slight modification in injection coordinates: 0.3 mm anterior and 1 mm lateral to bregma, and a depth of 3 mm.

Real-time reverse-transcription polymerase chain reaction.

Total RNA was isolated from mouse tissues and real-time reverse-transcription polymerase chain reaction (qRT-PCR) was performed as previously described (Rigo et al., 2014). Approximately 10 ng RNA was added to EXPRESS One-Step SuperScript qRT-PCR Kit (ThermoFisher, Waltham, MA) with Tagman primer and probe sets: *Epha4* forward primer, GAGTGTCTAAGTATAACCCTAGCC; *Epha4* reverse primer, TCTTTAGCCTGGACCAAAGC; *Epha4* probe, CAACCAACCAAGCAGCACCATCAT; *Gfap* forward primer, GAGAGAGATTCGCACTCAATACGA; *Gfap* reverse primer, GTCTGCAAACTTAGACCGATACCA; *Gfap* probe, CAGTGGCCACCAGTAACATGCAAGAGAC; *Gapdh* forward primer, GGCAAATTCAACGGCACAGT; *Gapdh* reverse primer, GGGTCTCGCTCCTGGAAGAT; *Gapdh* probe, AAGGCCGAGAATGGGAAGCTTGTCATC. The target gene expression was normalized to the housekeeping gene *Gapdh* and this was further normalized to the level in untreated mice.

Western blotting.

Tissues were homogenized with RIPA buffer supplemented with protease inhibitor. Protein extracts were supernatants of lysates subjected to centrifugation at 10,000 × g for 10 min at 4 °C. Total Protein (20–40 μg/lane) were separated by 4–12% SDS-PAGE gel and transferred to PVDF membrane. EphA4 and β-tubulin were detected with anti-EphA4 antibody (1:1000; AB_2533301, clone 4C8H5, ThermoFisher, Waltham, MA) and anti-β-tubulin antibody (1:5000; GE Healthcare Life Sciences, Pittsburgh, PA), respectively; followed by secondary antibodies and visualization using ECL. Mitochondrial cytochrome c oxidase (COX 4 or COX IV) expression in the gastrocnemius muscle was probed with anti-COX 4 antibody (AB_301443, Cat. # ab14744, Abcam, Cambridge, MA). Signal Intensities of corresponding protein bands were imaged and quantified with Bio-rad Gel Doc System (Bio-Rad, Hercules, CA).

Immunofluorescent staining and quantification of NMJ.

Tibialis anterior (TA) muscles were dissected and dropped fixed in 4% paraformaldehyde for 1 h. Muscles were embedded in Tissue Tek O.C.T. (Sakura Finetek, Torrance, CA), flash-frozen and sectioned (20 μm-thickness) on a cryostat. Cryosections were rinsed stained for neuromuscular junctions using anti-VAChT (1:200; synaptic system, Goettingen, Germany) in 5% goat serum/0.2% TritonX-100/phosphate buffered solution, followed by Alexa-fluor 488 conjugated goat anti-rabbit secondary antibody and Alexa-fluor 555 conjugated α-bungarotoxin (ThermoFisher, Waltham, MA; 1:1000). Fluorescently labeled NMJs were observed by epifluorescence or confocal microscopy. Fully innervated NMJs were defined by the complete overlap of presynaptic (i.e., VAChT) and post-synaptic (α-bungarotoxin) labeling. Illustrated images are flattened projections of Z-stack images acquired at sequential focal planes 1 μm apart using the Olympus confocal microscope.

Sciatic nerve injury.

Mice were anaesthetized with 2% isoflurane. Using a surgical aseptic technique, the sciatic nerve was freed from surrounding tissues and crushed twice with a super-fine hemostatic forcep (Fine Science Tools, 13020–12) for 15 seconds at 3 clicks. After the skin incision was sutured, animals were returned to their cage. The sham surgery followed the same procedure, except that the nerve was not crushed.

Behavioral tests.

For grip-strength analysis, mice were allowed to grasp with one hindlimb onto a horizontal pull bar of the grip strength meter (Columbus Instrument, 1027SM-D58). Once a stable grip was established, the mouse was slowly pulled from the bar until the grip was released and the maximum tension was recorded. Grip strength from each animal's hindlimb was averaged from 3 measurements. Functional recovery was assayed by measuring the grip strength of the injured (left) over sham (right) hindlimb. For rotarod analysis, an accelerating protocol (2–40 rpm/3 min) was used for $SOD1^{G93A}$mice and constant protocol (12 rpm/3 min) was used for $PFN1^{G118V}$ mice. Mice were placed on the rotarod (Ugo Basile #47600) and allowed to run for 3 min maximum per trial. The latency to fall was recorded from averaging 2 trials within the day. For the footprint analysis, hindpaws were painted with

water soluble non-toxic paint and mice were allowed to walk on a paper (50-cm in length). Stride lengths were computed from the average of 3 trials. Animals were returned to their cage after residual paint from the paws was removed.

Neurological and moribund assessment.

Animals were weighed at least once a week until 110 days, twice a week until 130 days and three times a week until the end of the study. At the time of weighing, the ALS TDI neurological scores (0–4) were assessed, with a score of 0 and 4 defined as normal and endpoint, respectively (Hatzipetros et al., 2015). Briefly, a full extension of hindlimbs similar to that of healthy mice was given score of 0. An acute angled splay towards the midline or trembling of hindlimbs received a score of 1. If any part of the foot was dragging the mouse received a score of 2. Rigid paralysis or minimal joint movement during forward motion was scored as a 3. Inability to right itself when placed on the animal's back in 15 s was scored as 4. Disease onset was retrospectively determined in two ways: 1) 10% drop in body weight, and; 2) the first observation of neurological score of 1 or more in 3 consecutive days. The moribund stage was defined by a neurological score of 4. The disease progression was measured by the length of time an individual animal survived after onset of neurological symptoms.

CMAP measurement.

Mice were anesthetized with under 2% isofluorane. The sciatic nerve was stimulated percutaneously by single pulses of 0.1 ms duration (VikingQuest NCS/EMG Portable EMG machine) delivered through a pair of needle electrodes placed subdermally at the sciatic notch. The CMAP was recorded with the recording electrode placed subdermally on the muscle belly of the tibialis anterior muscle. A reference electrode was placed near the ankle and the ground electrode at the animal's back near the midline. Disposable monopolar needle electrodes (25 mm, 28 G; catalog # 902-DMF25-TP, Natus Medical Inc., San Carlos, CA) were used for both stimulating and recording. The CMAP trace used for analysis from a given animal/leg was obtained from 4 supramaximal stimuli. The CMAP value of an individual animal at a given time point represents the averaged peak-to-peak amplitude of both left and right legs.

Quantitative real-time PCR of ALS samples.

Subjects with ALS were recruited as part of the EMPOWER clinical study assessing the activity of dexpramipexole in ALS. Samples were collected with informed consent and were taken prior to treatment with placebo or dexpramipexole. RNA was extracted from peripheral whole blood using PAXgene tubes and PAXgene extraction kit (Qiagen). We obtained quantitative real-time PCR expression data from total blood of 192 individuals with ALS, containing all blood cells including polymorphonuclear leukocytes, mononuclear cells, platelets and red blood cells. Five samples failed to provide a robust EphA4 measurement and were excluded. To perform quantitative real-time PCR, we used the Hs00177874_m1 assay against human EPHA4, the Hs99999905_m1 assay against human GAPDH (endogenous control, Applied Biosystems). Reverse transcription was performed using the High Capacity cDNA Archive kit (Applied Biosystems) and real-time PCR was

performed with Taqman universal PCR mastermix (Applied Biosystems) and the 7900HT (AB) Real-time PCR systems (Applied Biosystems).

RNAscope® in-situ hybridization and data acquisition.

Spinal cord tissues were dissected, fixed in 10% neutral formalin for 2 days and subsequently switched to 70% ethanol for 3 days. Samples were paraffin embeded, sectioned at 4 μm thickness and mounted on slides. *Epha4* and *Rbfox3* mRNA were detected with RNAscope® 2.5 LS Probe- Mm-Epha4 (Cat No. 419088, Advanced Cell Diagnostic, CA) and RNAscope® 2.5 LS Probe- Mm-Rbfox3-C2 (Cat No. 313318-C2, Advanced Cell Diagnostic, CA), respectively, using RNAscope® LS multiplex fluorescent reagent kit. Images of all samples were acquired using EVOS Cell Imaging System (Thermo Fisher Scientific, CA) with a 20X objective at same exposures and gain. For analysis, neuronal boundaries were manually defined in bright field images. Fluorescent intensity of individual *Rbfox3*-positive neurons normalized to cell size were measured by imageJ. Ventral horn neurons >360 μm^2 were defined as alpha motor neurons (Friese et al., 2009).

Supplementary Material

Refer to Web version on PubMed Central for supplementary material.

Acknowledgments

This work was supported by Biogen and Ionis Pharmaceuticals. M.K. gratefully acknowledges the support by National Institute of Neurological Disorders and Stroke NS088653 and by grants from the University of Arkansas for Medical Sciences Startup Fund, Pepper Center Pilot Award, University of Arkansas for Medical Sciences Center for Translational Neurosciences, National Institute of General Medical Sciences IDeA Program Award P30 GM110702, P20GM109005.

References

Al-Chalabi A, van den Berg LH, Veldink J, 2017. Gene discovery in amyotrophic lateral sclerosis: implications for clinical management. Nat Rev Neurol. 13, 96–104. [PubMed: 27982040]

Bros-Facer V, Krull D, Taylor A, Dick JR, Bates SA, Cleveland MS, Prinjha RK, Greensmith L, 2014. Treatment with an antibody directed against Nogo-A delays disease progression in the SOD1G93A mouse model of Amyotrophic lateral sclerosis. Hum Mol Genet. 23, 4187–4200. [PubMed: 24667415]

Bruneteau G, Bauche S, Gonzalez de Aguilar JL, Brochier G, Mandjee N, Tanguy ML, Hussain G, Behin A, Khiami F, Sariali E, Hell-Remy C, Salachas F, Pradat PF, Lacomblez L, Nicole S, Fontaine B, Fardeau M, Loeffler JP, Meininger V, Fournier E, Koenig J, Hantai D, 2015. Endplate denervation correlates with Nogo-A muscle expression in amyotrophic lateral sclerosis patients. Ann Clin Transl Neurol. 2, 362–372. [PubMed: 25909082]

De Winter F, Vo T, Stam FJ, Wisman LA, Bar PR, Niclou SP, van Muiswinkel FL, Verhaagen J, 2006. The expression of the chemorepellent Semaphorin 3A is selectively induced in terminal Schwann cells of a subset of neuromuscular synapses that display limited anatomical plasticity and enhanced vulnerability in motor neuron disease. Mol Cell Neurosci. 32, 102–117. [PubMed: 16677822]

DeVos SL, Goncharoff DK, Chen G, Kebodeaux CS, Yamada K, Stewart FR, Schuler DR, Maloney SE, Wozniak DF, Rigo F, Bennett CF, Cirrito JR, Holtzman DM, Miller TM, 2013. Antisense reduction of tau in adult mice protects against seizures. J Neurosci. 33, 12887–12897. [PubMed: 23904623]

DeVos SL, Miller RL, Schoch KM, Holmes BB, Kebodeaux CS, Wegener AJ, Chen G, Shen T, Tran H, Nichols B, Zanardi TA, Kordasiewicz HB, Swayze EE, Bennett CF, Diamond MI, Miller TM,

2017. Tau reduction prevents neuronal loss and reverses pathological tau deposition and seeding in mice with tauopathy. Sci Transl Med. 9, 10.1126/scitranslmed.aag0481

Faruqi M, 2012. Neurodegenerative disease: EPHA4 inhibition rescues neurodegeneration in ALS. Nat Rev Drug Discov. 11, 747. [PubMed: 23023674]

Fil D, DeLoach A, Yadav S, Alkam D, MacNicol M, Singh A, Compadre CM, Goellner JJ, O'Brien CA, Fahmi T, Basnakian AG, Calingasan NY, Klessner JL, Beal FM, Peters OM, Metterville J, Brown RH Jr., Ling KKY, Rigo F, Ozdinler PH, Kiaei M, 2017. Mutant Profilin1 transgenic mice recapitulate cardinal features of motor neuron disease. Hum Mol Genet. 26, 686–701. [PubMed: 28040732]

Friese A, Kaltschmidt JA, Ladle DR, Sigrist M, Jessell TM, Arber S, 2009. Gamma and alpha motor neurons distinguished by expression of transcription factor Err3. Proc Natl Acad Sci U S A. 106, 13588–13593. [PubMed: 19651609]

Frugier T, Conquest A, McLean C, Currie P, Moses D, Goldshmit Y, 2012. Expression and activation of EphA4 in the human brain after traumatic injury. J Neuropathol Exp Neurol. 71, 242–250. [PubMed: 22318127]

Geuna S, Raimondo S, Fregnan F, Haastert-Talini K, Grothe C, 2016. In vitro models for peripheral nerve regeneration. Eur J Neurosci. 43, 287–296. [PubMed: 26309051]

Goldshmit Y, Galea MP, Wise G, Bartlett PF, Turnley AM, 2004. Axonal regeneration and lack of astrocytic gliosis in EphA4-deficient mice. J Neurosci. 24, 10064–10073. [PubMed: 15537875]

Goldshmit Y, McLenachan S, Turnley A, 2006. Roles of Eph receptors and ephrins in the normal and damaged adult CNS. Brain Res Rev. 52, 327–345. [PubMed: 16774788]

Goldshmit Y, Spanevello MD, Tajouri S, Li L, Rogers F, Pearse M, Galea M, Bartlett PF, Boyd AW, Turnley AM, 2011. EphA4 blockers promote axonal regeneration and functional recovery following spinal cord injury in mice. PLoS One. 6, e24636. [PubMed: 21931787]

Gurney ME, 1997. The use of transgenic mouse models of amyotrophic lateral sclerosis in preclinical drug studies. J Neurol Sci. 152 Suppl 1, S67–73. [PubMed: 9419057]

Gurney ME, Pu H, Chiu AY, Dal Canto MC, Polchow CY, Alexander DD, Caliendo J, Hentati A, Kwon YW, Deng HX, et al. , 1994. Motor neuron degeneration in mice that express a human Cu,Zn superoxide dismutase mutation. Science. 264, 1772–1775. [PubMed: 8209258]

Hatzipetros T, Kidd JD, Moreno AJ, Thompson K, Gill A, Vieira FG, 2015. A Quick Phenotypic Neurological Scoring System for Evaluating Disease Progression in the SOD1-G93A Mouse Model of ALS. J Vis Exp. 10.3791/53257.

Heiman-Patterson TD, Deitch JS, Blankenhorn EP, Erwin KL, Perreault MJ, Alexander BK, Byers N, Toman I, Alexander GM, 2005. Background and gender effects on survival in the TgN(SOD1-G93A)1Gur mouse model of ALS. J Neurol Sci. 236, 1–7. [PubMed: 16024047]

Johnston CA, Stanton BR, Turner MR, Gray R, Blunt AH, Butt D, Ampong MA, Shaw CE, Leigh PN, Al-Chalabi A, 2006. Amyotrophic lateral sclerosis in an urban setting: a population based study of inner city London. J Neurol. 253, 1642–1643. [PubMed: 17219036]

Jokic N, Gonzalez de Aguilar JL, Dimou L, Lin S, Fergani A, Ruegg MA, Schwab ME, Dupuis L, Loeffler JP, 2006. The neurite outgrowth inhibitor Nogo-A promotes denervation in an amyotrophic lateral sclerosis model. EMBO Rep. 7, 1162–1167. [PubMed: 17039253]

Jokic N, Gonzalez de Aguilar JL, Pradat PF, Dupuis L, Echaniz-Laguna A, Muller A, Dubourg O, Seilhean D, Hauw JJ, Loeffler JP, Meininger V, 2005. Nogo expression in muscle correlates with amyotrophic lateral sclerosis severity. Ann Neurol. 57, 553–556. [PubMed: 15786457]

Joly S, Jordi N, Schwab ME, Pernet V, 2014. The Ephrin receptor EphA4 restricts axonal sprouting and enhances branching in the injured mouse optic nerve. Eur J Neurosci. 40, 3021–3031. [PubMed: 25041248]

Kempf A, Montani L, Petrinovic MM, Schroeter A, Weinmann O, Patrignani A, Schwab ME, 2013. Upregulation of axon guidance molecules in the adult central nervous system of Nogo-A knockout mice restricts neuronal growth and regeneration. Eur J Neurosci. 38, 3567–3579. [PubMed: 24103058]

Klein R, 2012. Eph/ephrin signalling during development. Development. 139, 4105–4109. [PubMed: 23093422]

Klein R, Kania A, 2014. Ephrin signalling in the developing nervous system. Curr Opin Neurobiol. 27, 16–24. [PubMed: 24608162]

Kordasiewicz HB, Stanek LM, Wancewicz EV, Mazur C, McAlonis MM, Pytel KA, Artates JW, Weiss A, Cheng SH, Shihabuddin LS, Hung G, Bennett CF, Cleveland DW, 2012. Sustained therapeutic reversal of Huntington's disease by transient repression of huntingtin synthesis. Neuron. 74, 1031–1044. [PubMed: 22726834]

Lai KO, Ip NY, 2009. Synapse development and plasticity: roles of ephrin/Eph receptor signaling. Curr Opin Neurobiol. 19, 275–283. [PubMed: 19497733]

Lemmens R, Jaspers T, Robberecht W, Thijs VN, 2013. Modifying expression of EphA4 and its downstream targets improves functional recovery after stroke. Hum Mol Genet. 22, 2214–2220. [PubMed: 23418304]

Lowery LA, Van Vactor D, 2009. The trip of the tip: understanding the growth cone machinery. Nat Rev Mol Cell Biol. 10, 332–343. [PubMed: 19373241]

Meininger V, Genge A, van den Berg LH, Robberecht W, Ludolph A, Chio A, Kim SH, Leigh PN, Kiernan MC, Shefner JM, Desnuelle C, Morrison KE, Petri S, Boswell D, Temple J, Mohindra R, Davies M, Bullman J, Rees P, Lavrov A, Group NOGS, 2017. Safety and efficacy of ozanezumab in patients with amyotrophic lateral sclerosis: a randomised, double-blind, placebo-controlled, phase 2 trial. Lancet Neurol. 16, 208–216. [PubMed: 28139349]

Murai KK, Nguyen LN, Irie F, Yamaguchi Y, Pasquale EB, 2003a. Control of hippocampal dendritic spine morphology through ephrin-A3/EphA4 signaling. Nat Neurosci. 6, 153–160. [PubMed: 12496762]

Murai KK, Nguyen LN, Koolpe M, McLennan R, Krull CE, Pasquale EB, 2003b. Targeting the EphA4 receptor in the nervous system with biologically active peptides. Mol Cell Neurosci. 24, 1000–1011. [PubMed: 14697664]

Murai KK, Pasquale EB, 2005. New exchanges in eph-dependent growth cone dynamics. Neuron. 46, 161–163. [PubMed: 15848793]

Overman JJ, Clarkson AN, Wanner IB, Overman WT, Eckstein I, Maguire JL, Dinov ID, Toga AW, Carmichael ST, 2012. A role for ephrin-A5 in axonal sprouting, recovery, and activity-dependent plasticity after stroke. Proc Natl Acad Sci U S A. 109, E2230–2239. [PubMed: 22837401]

Peters MJ, Joehanes R, Pilling LC, Schurmann C, Conneely KN, Powell J, Reinmaa E, Sutphin GL, Zhernakova A, Schramm K, Wilson YA, Kobes S, Tukiainen T, Consortium NU, Ramos YF, Goring HH, Fornage M, Liu Y, Gharib SA, Stranger BE, De Jager PL, Aviv A, Levy D, Murabito JM, Munson PJ, Huan T, Hofman A, Uitterlinden AG, Rivadeneira F, van Rooij J, Stolk L, Broer L, Verbiest MM, Jhamai M, Arp P, Metspalu A, Tserel L, Milani L, Samani NJ, Peterson P, Kasela S, Codd V, Peters A, Ward-Caviness CK, Herder C, Waldenberger M, Roden M, Singmann P, Zeilinger S, Illig T, Homuth G, Grabe HJ, Volzke H, Steil L, Kocher T, Murray A, Melzer D, Yaghootkar H, Bandinelli S, Moses EK, Kent JW, Curran JE, Johnson MP, Williams-Blangero S, Westra HJ, McRae AF, Smith JA, Kardia SL, Hovatta I, Perola M, Ripatti S, Salomaa V, Henders AK, Martin NG, Smith AK, Mehta D, Binder EB, Nylocks KM, Kennedy EM, Klengel T, Ding J, Suchy-Dicey AM, Enquobahrie DA, Brody J, Rotter JI, Chen YD, Houwing-Duistermaat J, Kloppenburg M, Slagboom PE, Helmer Q, den Hollander W, Bean S, Raj T, Bakhshi N, Wang QP, Oyston LJ, Psaty BM, Tracy RP, Montgomery GW, Turner ST, Blangero J, Meulenbelt I, Ressler KJ, Yang J, Franke L, Kettunen J, Visscher PM, Neely GG, Korstanje R, Hanson RL, Prokisch H, Ferrucci L, Esko T, Teumer A, van Meurs JB, Johnson AD, 2015. The transcriptional landscape of age in human peripheral blood. Nat Commun. 6, 8570. [PubMed: 26490707]

Reddy LV, Miller TM, 2015. RNA-targeted Therapeutics for ALS. Neurotherapeutics. 12, 424–427. [PubMed: 25753730]

Renton AE, Chio A, Traynor BJ, 2014. State of play in amyotrophic lateral sclerosis genetics. Nat Neurosci. 17, 17–23. [PubMed: 24369373]

Rigo F, Chun SJ, Norris DA, Hung G, Lee S, Matson J, Fey RA, Gaus H, Hua Y, Grundy JS, Krainer AR, Henry SP, Bennett CF, 2014. Pharmacology of a central nervous system delivered 2'-O-methoxyethyl-modified survival of motor neuron splicing oligonucleotide in mice and nonhuman primates. J Pharmacol Exp Ther. 350, 46–55. [PubMed: 24784568]

Swayze EE, Siwkowski AM, Wancewicz EV, Migawa MT, Wyrzykiewicz TK, Hung G, Monia BP, Bennett CF, 2007. Antisense oligonucleotides containing locked nucleic acid improve potency but cause significant hepatotoxicity in animals. Nucleic Acids Res. 35, 687–700. [PubMed: 17182632]

Taylor JP, Brown RH Jr., Cleveland DW, 2016. Decoding ALS: from genes to mechanism. Nature. 539, 197–206. [PubMed: 27830784]

Van Hoecke A, Schoonaert L, Lemmens R, Timmers M, Staats KA, Laird AS, Peeters E, Philips T, Goris A, Dubois B, Andersen PM, Al-Chalabi A, Thijs V, Turnley AM, van Vught PW, Veldink JH, Hardiman O, Van Den Bosch L, Gonzalez-Perez P, Van Damme P, Brown RH Jr., van den Berg LH, Robberecht W, 2012. EPHA4 is a disease modifier of amyotrophic lateral sclerosis in animal models and in humans. Nat Med. 18, 1418–1422. [PubMed: 22922411]

Venkova K, Christov A, Kamaluddin Z, Kobalka P, Siddiqui S, Hensley K, 2014. Semaphorin 3A signaling through neuropilin-1 is an early trigger for distal axonopathy in the SOD1G93A mouse model of amyotrophic lateral sclerosis. J Neuropathol Exp Neurol. 73, 702–713. [PubMed: 24918638]

Wu B, De SK, Kulinich A, Salem AF, Koeppen J, Wang R, Barile E, Wang S, Zhang D, Ethell I, Pellecchia M, 2017. Potent and Selective EphA4 Agonists for the Treatment of ALS. Cell Chem Biol. 24, 293–305. [PubMed: 28196613]

Wu CH, Fallini C, Ticozzi N, Keagle PJ, Sapp PC, Piotrowska K, Lowe P, Koppers M, McKenna-Yasek D, Baron DM, Kost JE, Gonzalez-Perez P, Fox AD, Adams J, Taroni F, Tiloca C, Leclerc AL, Chafe SC, Mangroo D, Moore MJ, Zitzewitz JA, Xu ZS, van den Berg LH, Glass JD, Siciliano G, Cirulli ET, Goldstein DB, Salachas F, Meininger V, Rossoll W, Ratti A, Gellera C, Bosco DA, Bassell GJ, Silani V, Drory VE, Brown RH Jr., Landers JE, 2012. Mutations in the profilin 1 gene cause familial amyotrophic lateral sclerosis. Nature. 488, 499–503. [PubMed: 22801503]

Highlights

- CNS-directed reduction of EphA4 by antisense oligonucleotides is sufficient to promote axonal regeneration of the sciatic nerve after injury in mice.
- CNS-directed reduction of EphA4 by antisense oligonucleotides provides no benefits in survival of mouse models of ALS with $SOD1^{G93A}$ or $PFN1^{G118V}$ mutations.
- *EPHA4* mRNA level in blood does not predict the rate of disease progression measured by ALSFRS.

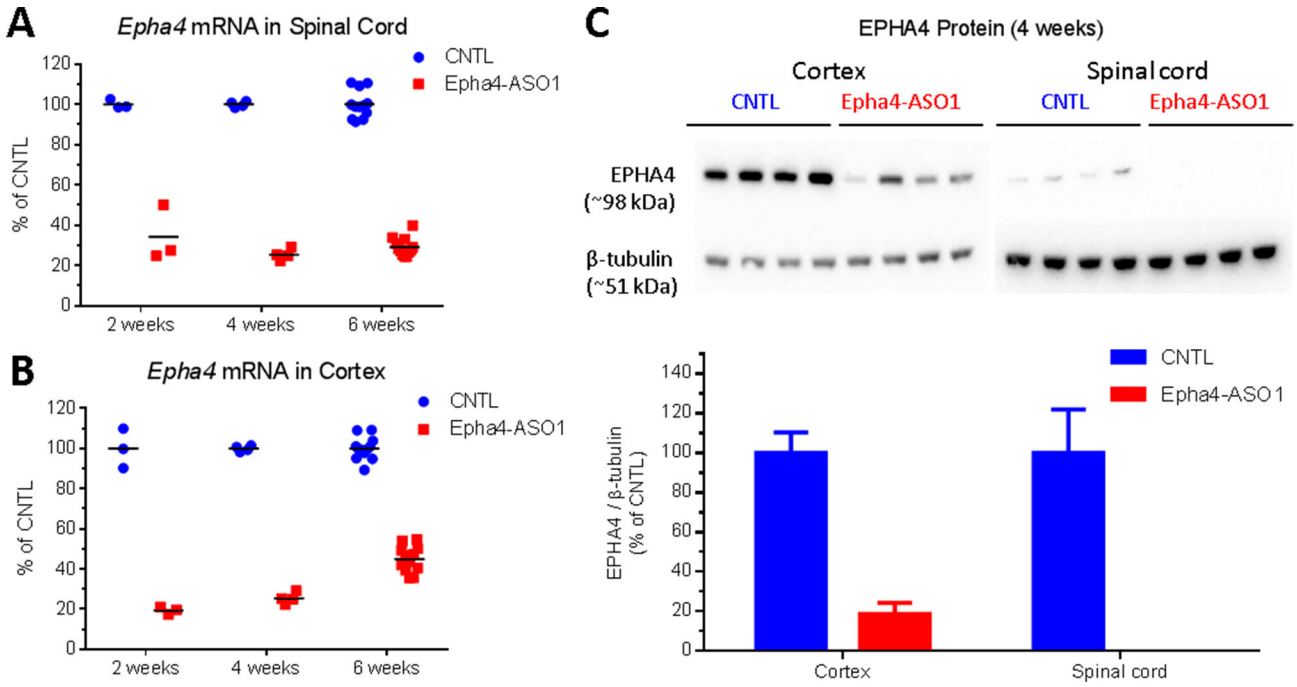

Figure 1: Reduction of *Epha4* mRNA and protein in the CNS of mice by Epha4-ASO treatment

(A-B) *Epha4* mRNA in cortex and spinal cord of mice at 2–6 weeks after receiving a single intracerebroventricular injection of 500 μg Epha4-ASO1 or vehicle. $p < 0.0001$, two-way ANOVA. (C) Western blots and quantification of EPHA4 protein in cortex and spinal cord of mice 4 weeks after Epha4-ASO treatment. $n = 4$ and data is mean ± SEM. $p < 0.002$, unpaired *t-test.*

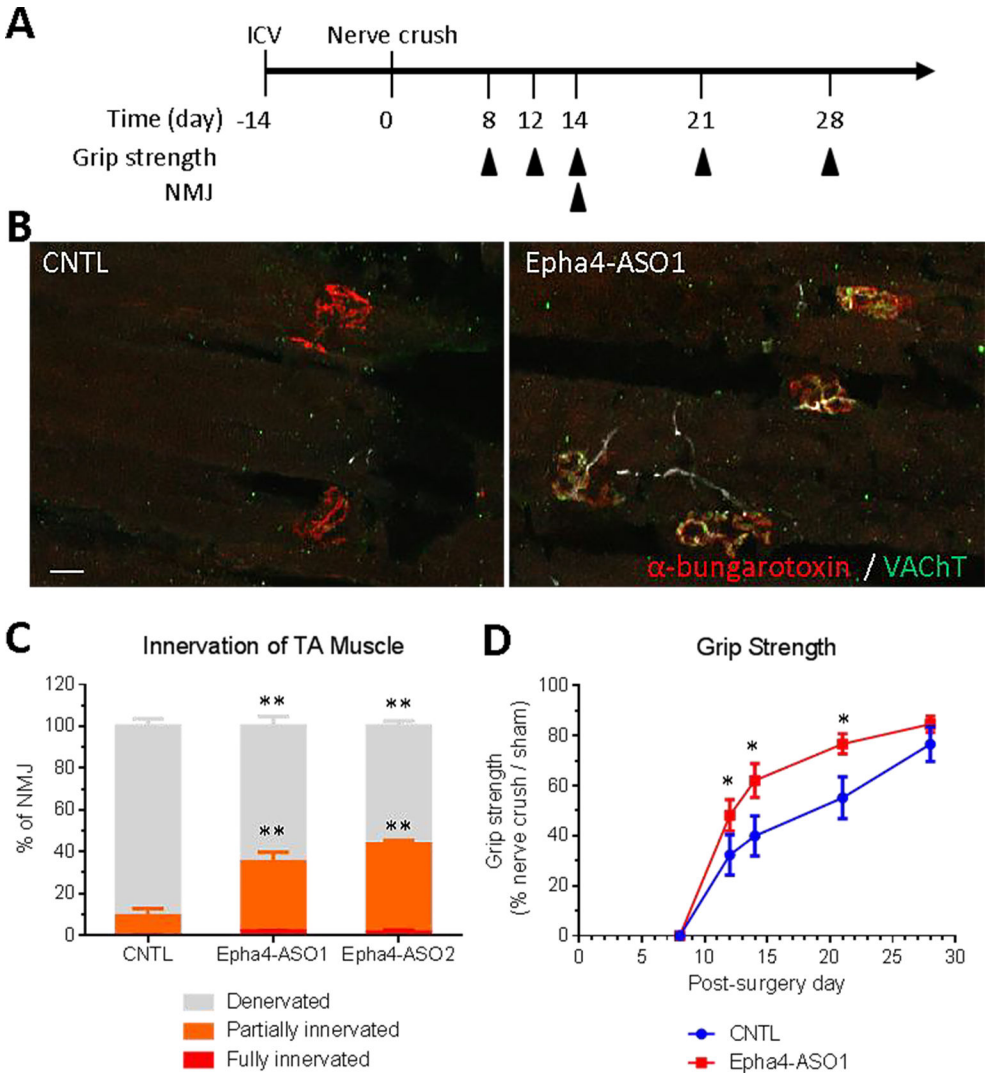

Figure 2: Epha4-ASOs improve NMJ re-innervation and functional recovery after sciatic nerve crush

(A) Experimental timeline for sciatic nerve crush injury and NMJ analyses in wild type mice injected with Epha4-ASOs or vehicle. (B-C) Confocal images of NMJs in tibialis anterior (TA) muscles of mice injected with vehicle (CNTL) and Epha4-ASO at 2 weeks after sciatic nerve crush. α-bungarotoxin (red) and VAChT (green) labels post-synaptic and presynaptic nerve specialization respectively. Scale bar, 20 μm. (C) Quantification of NMJ innervation in TA muscles of CNTL and Epha4-ASOs-treated mice at 2 weeks after sciatic nerve crush. n = 4 and data is mean ± SEM. Denervated NMJ, $F(2,6)=22.98$, **p=0.0015; Partially innervated NMJ, $F(2,6)=24.16$, **p=0.0013; Fully innervated, $F(2,6)=2.335$, p=0.1778, One-way ANOVA followed by Dunnet's multiple comparisons. (D) Recovery of grip strength presented as % of grip strength of hindlimb subjected to nerve crush over sham surgery in wild type mice treated with vehicle control (n = 11) or Epha4-ASO1 (n = 12). Data is mean ± SEM. *p = 0.047, two-way ANOVA analysis of post-surgery days 12, 14 and 21.

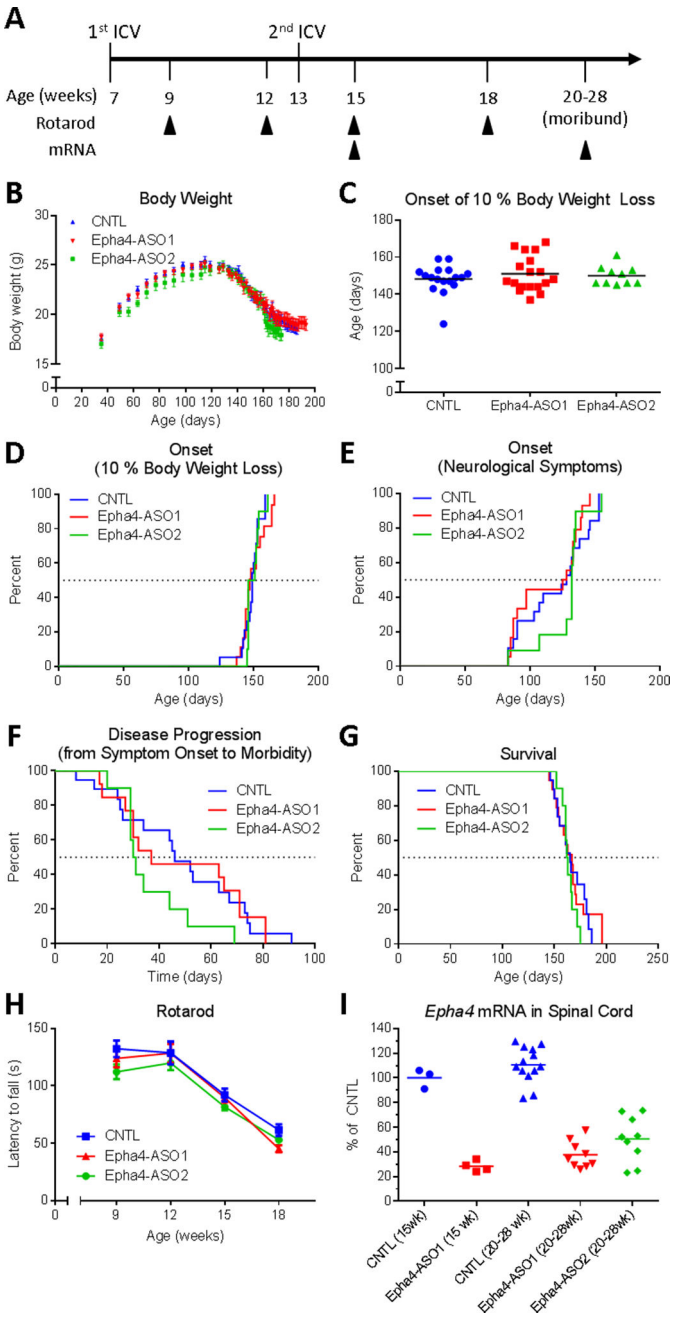

Figure 3: Epha4-ASO treatment does not affect body weight, disease progression, survival and motor performance of SOD1^{G93A} mice

(A) Experimental timeline for survival, behavioral and mRNA expression analyses of SOD1^{G93A} mice injected with Epha4-ASOs or vehicle. Data is mean ± SEM. (B) Body weight measurement of SOD1^{G93A} mice treated with vehicle CNTL (n = 17), Epha4-ASO1 (n = 17) or Epha4-ASO2 (n = 10). (C) Average age of CNTL-or ASO-treated SOD1^{G93A} mice displaying 10% of body weight loss (CNTL, 148.2 ± 1.9 g; Epha4-ASO1, 150.9 ± 2.2 g; Epha4-ASO2, 150.0 ± 1.6 g; p = 0.60, one-way ANOVA). (D-G) Kaplan-Meier analyses of onset of weight loss (median: CNTL, 149 days; Epha4-ASO1, 147 days; Epha4-ASO2, 148.5 days), onset of neurological symptoms (median: CNTL, 128 days; Epha4-ASO1, 127

days; Epha4-ASO2, 132 days), disease progression from onset of neurological symptoms to morbidity (median: CNTL, 46 days; Epha4-ASO1, 37 days; Epha4-ASO2, 31 days) and survival (median: CNTL, 165 days; Epha4-ASO1, 167 days; Epha4-ASO2, 163 days) of CNTL-or ASO-treated $SOD1^{G93A}$ mice. (H) Rotarod analysis of $SOD1^{G93A}$ mice treated with vehicle CNTL (n = 17), Epha4-ASO1 (n = 17) or Epha4-ASO2 (n = 10). Data is mean ± SEM. (I) *Epha4* mRNA expression in spinal cord of CNTL-or ASO-treated $SOD1^{G93A}$ mice at 15 weeks and moribund stage (20–28 weeks); $p < 0.0001$, two-way ANOVA.

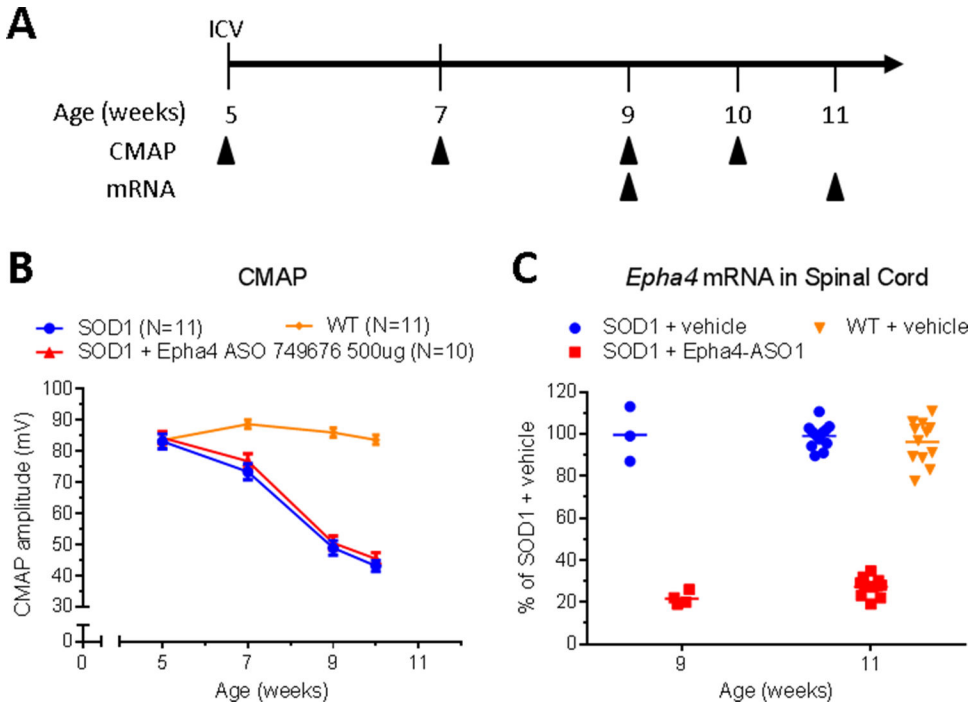

Figure 4: Epha4-ASO treatment does not ameliorate the loss of CMAP in SOD1^{G93A} mice despite robust reduction in *Epha4* mRNA

(A) Experimental timeline for CMAP and mRNA expression analyses of SOD1^{G93A} mice injected with Epha4-ASO1 or vehicle. (B) Average CMAP amplitude of SOD1^{G93A} mice treated with Epha4-ASO1 (n = 10) or vehicle (n = 11), and wildtype littermates treated with vehicle (n = 11). Data is mean ± SEM. Epha4-ASO1 vs vehicle: p = 0.372, two-way ANOVA. (C) *Epha4* mRNA expression of SOD1^{G93A} mice or WT littermates treated with Epha4-ASO1 or vehicle at 9 and 11 weeks of age.

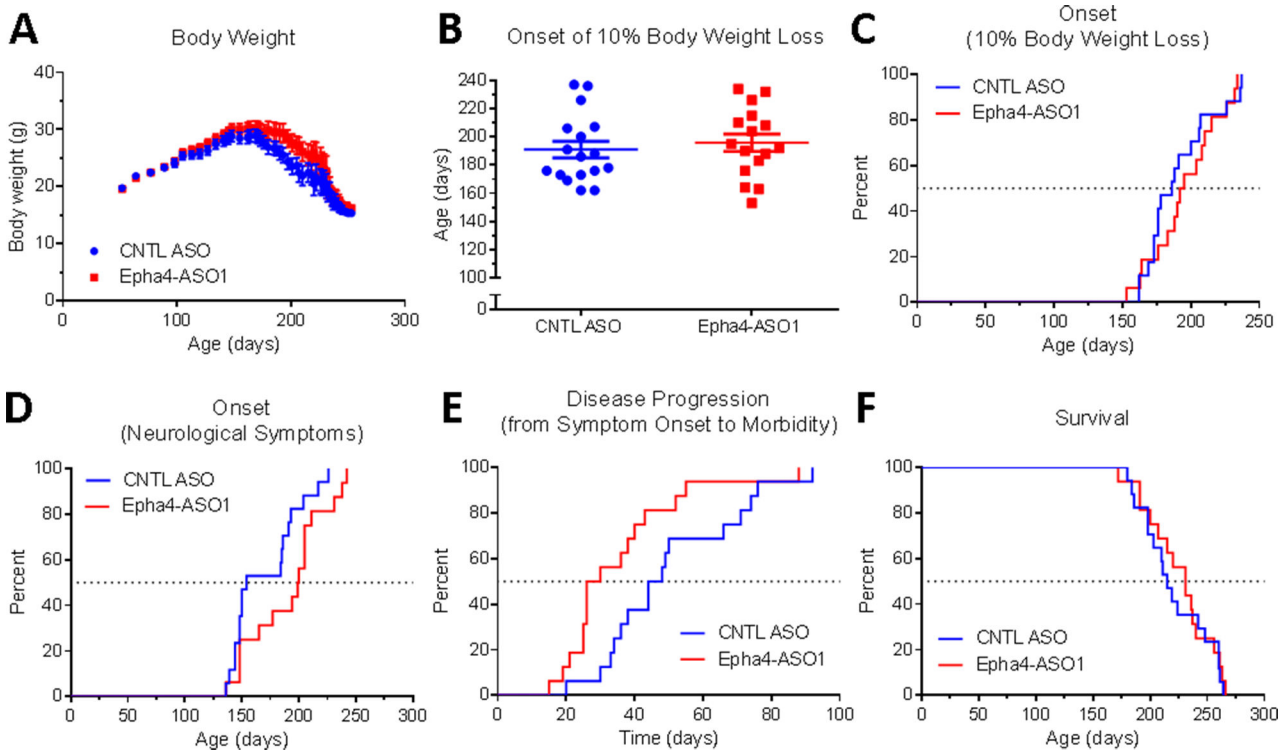

Figure 5: Epha4-ASO treatment does not improve disease progression and survival in PFN1^{G118V} mice

(A) Body weight measurement of PFN1^{G118V} mice treated with CNTL (n = 17) or Epha4-ASO1 (n = 16). (B) Average age of CNTL-or ASO-treated PFN1^{G118V} mice displaying 10% of body weight loss (CNTL: 190.9 ± 5.9 days vs Epha4-ASO1: 195.8 ± 6.1 days; data is mean ± SEM. p = 0.57, unpaired *t-test*). (C-F) Kaplan-Meier analyses of weight loss (median: CNTL, 186 days; Epha4-ASO1, 193 days; p = 0.853, log-rank (Mantel-Cox) test), disease onset (median, CNTL, 154 days; Epha4-ASO1, 200 days, p = 0.034, log-rank (Mantel-Cox) test), disease progression (median, CNTL, 46 days; Epha4-ASO1, 28 days, p = 0.056, log-rank (Mantel-Cox) test) and survival (median, CNTL, 215 days; Epha4-ASO1, 231 days, p = 0.569, log-rank (Mantel-Cox) test) comparing PFN1^{G118V} mice treated with CNTL- or Epha4-ASO1.

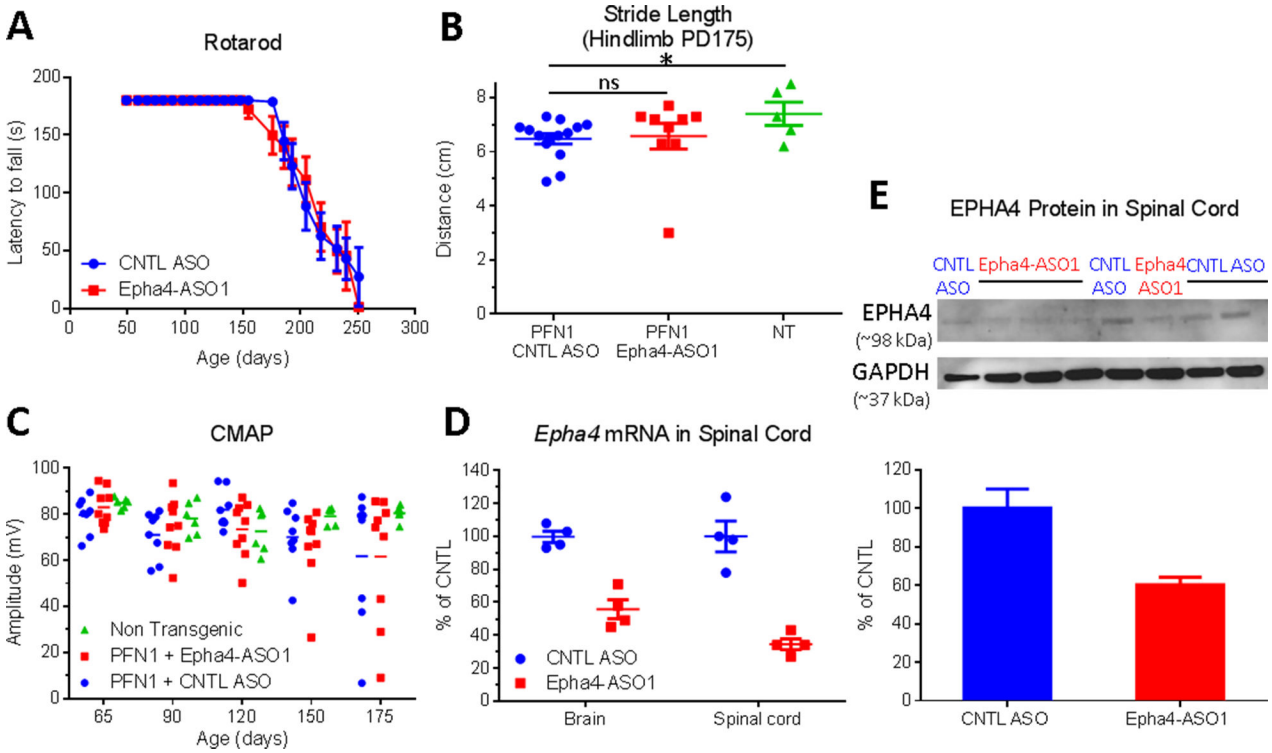

Figure 6: Epha4-ASO treatment does not improve motor function in PFN1^{G118V} mice

(A) Rotarod analysis of PFN1^{G118V} mice treated with CNTL ASO or Epha4-ASO1. (B) Stride length of CNTL ASO- (n = 17) or Epha4-ASO1 (n = 16) treated PFN1^{G118V} mice at post-natal day 175. WT vs PFN1^{G118V}+ CNTL-ASO, p=0.037, unpaired t-test. (C) Average CMAP amplitude of tibialis muscle of non-transgenic mice or PFN1^{G118V} mice treated with CNTL ASO or Epha4-ASO1. (D) *Epha4* mRNA in brain and spinal cord of CNTL ASO- (n = 17) or Epha4-ASO1-(n = 16) treated PFN1^{G118V} mice at moribund stage. (E) Western blot and quantification of EPHA4 protein in spinal cord of CNTL ASO- or Epha4-ASO1-treated PFN1^{G118V} mice at moribund stage. n = 4 and data is mean ± SEM.

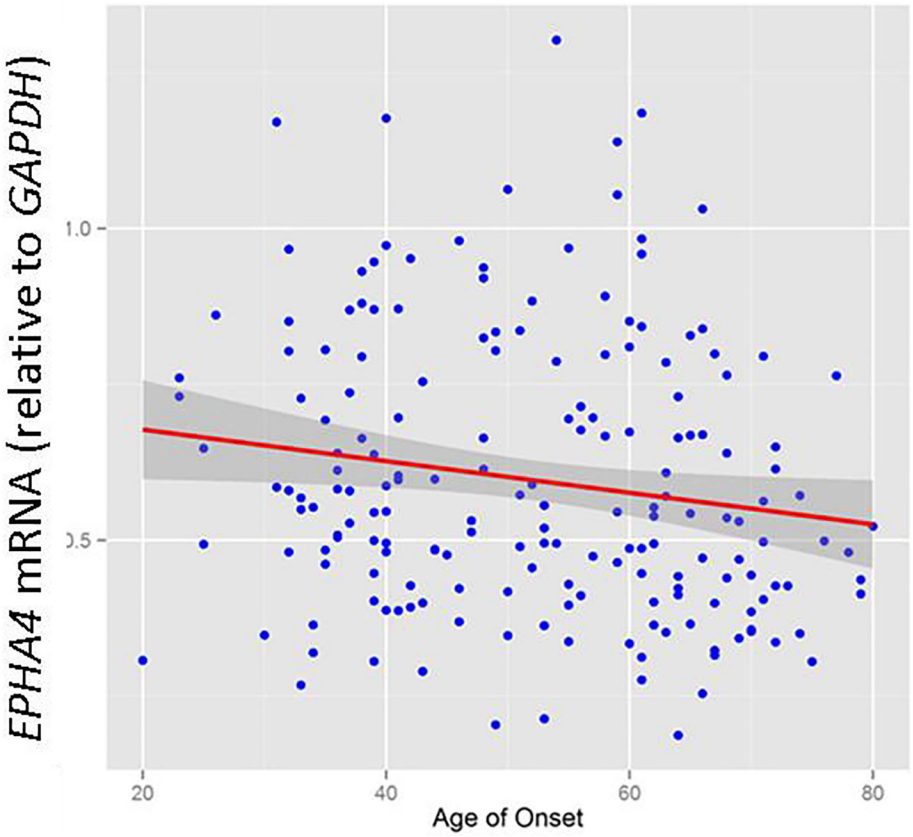

Figure 7: EPHA4 transcript in whole blood decreases with age of onset for ALS

EPHA4 mRNA in whole blood decreases relative to age of onset ($p < 0.05$; $r^2 = 0.026$) in ALS patients. *EPHA4* was quantified by qRT-PCR and is plotted relative to *GAPDH* mRNA levels.

Table 1:

Patient demographics for *EPHA4* mRNA analysis

Variable	Female	Male	Overall
Sex (%)	66 (35.3)	121 (64.7)	187 (100)
Death (%)	7 (10.6)	17 (14.0)	24 (12.8)
Bulbar onset (%)	17 (25.8)	17 (14.0)	34 (18.2)
Age onset: mean (sd)	55.7 (13.0)	49.9 (14.5)	51.9 (14.2)
EPHA4: mean (sd)	0.7 (0.2)	0.6 (0.2)	0.6 (0.2)
ALSFRS: mean (sd)	36.8 (5.6)	38.2 (5.8)	37.7 (5.8)
SYMPDUR: mean (sd)	16.4 (5.7)	14.7 (5.3)	15.3 (5.5)
Month DX: mean (sd)	6.9 (4.2)	7.5 (5.0)	7.3 (4.7)

The patient information for the samples in the *EPHA4* analysis is separated by gender.

Table 2:

Linear mixed model estimate of each variable on rate of progression of ALSFRS

	Estimate	S.E.	P-value
EPHA4 level	0.0042	0.0121	0.7265
Age of onset	−0.0130	0.0047	0.0062
SYMPDUR	0.0547	0.0128	<0.0001
BALSFRS	0.0495	0.0125	<0.0001
Sex (M)	0.0101	0.1432	0.9437

Age of onset, symptom duration (SYMDUR), and baseline ALSFRS (BALSFRS) are significant factors for predicting rate of disease progression. *EPHA4* level and gender were not.